FITTING THE GENERIC MULTI-PARAMETER CROSS-OVER MODEL: TOWARDS REALISTIC SCALING ESTIMATES

Z.R. STRUZIK, E.H. DOOIJES, F.C.A. GROEN
Faculty of Mathematics, Computer Science, Physics and Astronomy
University of Amsterdam, Kruislaan 403, 1098 SJ Amsterdam, The Netherlands

The primary concern of fractal metrology is providing a means of reliable estimation of scaling exponents such as fractal dimension, in order to prove the null hypothesis that a particular object can be regarded as fractal. In the particular context to be discussed in this contribution, the central question is what is the minimum extent of the scaling range needed to give any meaning to the object's description as a fractal. Preceded by a short review of the motivations for the generic transition model, we present the straightforward manner of extending it over more free parameters. The price paid for fitting such a multi-parametric model is, however, not only computational expense but the danger of obtaining far from optimal fits. Deterministic cross-sections through the parameter space of the model are demonstrated to show insight into the sensitivity of the fitting procedure to parameter variations. Realistic confidence intervals obtained are demonstrated to allow for testing the fractality hypothesis on the base of globally uniform scaling (fractal dimension). This is demonstrated in both examples of non-linear fit to measurements on decreasingly lowered generation level deterministic pre-fractals and genuine human writing samples.

1 Introduction: Finite Scales and Cross-over Models

It requires no lengthy argument to show that real world samples of fractals exhibit scaling over a limited range of scales (we will refer to such objects as pre-fractals). The breakdown of the scaling mechanism at some critical scale ω_{crit} must lead to transition from the fractal to the Euclidean region. This effect pertains both at the lower scale of fine detail as well as the upper scale of available sample.

Except for the cases of experimental difficulty of reaching scales smaller than the breakdown scale ω_{min} (or removal of what is often arbitrarily assumed as 'bad data'), one will always observe the effect of the departure from fractal scaling on the measurement data at small scales.

Although this is also the most often observed cross-over phenomenon, breakdown of the scaling around ω_{max}, i.e. at the upper scale determined by the available sample size, is just as obvious for real-life samples. Neglecting its existence cannot be justified by only considering the theoretical limit of the small scales in the determination of the scaling exponent; this is in practice infeasible and never done, precisely due to the above-mentioned finite sample size.

This issue would constitute little problem if the transition between the fractal and the Euclidean region was pointwise located in scale:

$$Ideal_{bound}(X) = \begin{cases} b\,X & for \quad X > 0 \\ 0 & for \quad X \leq 0\,. \end{cases} \tag{1}$$

Such an idealised crossover is, however, never observed in practice. Instead a variety of behaviours can be identified in the cross-over region, often relevant to the physics of the investigated phenomena or, in case of model fractal objects, to their geometry. A simple generic case for a transition model is illustrated in Fig. 1.

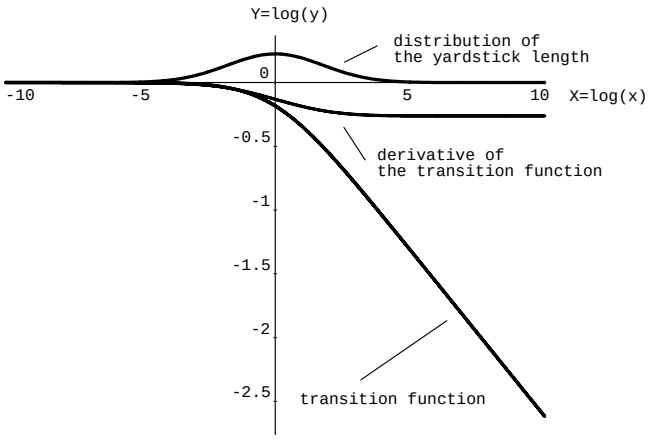

Figure 1: Here we plot the cross-over function which results from the convolution of the Gaussian distribution with the ideal transition.

The transition function with a smooth, continuously changing derivative, requires the fractal dimension to be defined locally in scale. [1] Assume we take the function $x/(1+x)$ as the model of smooth transition between dimension regimes (1 for $x \to \infty$, and 0 for $x \to 0$), as usual x is the scale or yardstick length. Adapting this transition to fractional dimensions is immediate, we will use $b = 1 - D$ to denote the dimensional increase where D is the fractal dimension, and 1 stands for the topological dimension of the investigated object in our case. (Extension to different topological dimensions is obvious and does not influence the generality of the following considerations.) Thus the suggested transition model in logarithmic coordinates ($X = log(x)$, $Y = log(y)$) reads:

$$Y_b \sim b \, (\frac{e^X}{1+e^X}) \, .$$

This model features a fixed transition rate as well as the effective extent of the cross-over.[a] However extending it is a matter of a rescaling operation $X \to a \, X$ with parameter $a > 0$:

$$Y_{a,b} \sim b \, (\frac{e^{aX}}{1+e^{aX}}) \, .$$

The corresponding model for the measurement data can be shown [1] to be

$$y = y_0 \, (x^a + x_c^a)^{b/a} \, , \tag{2}$$

where x_c is the transition point and y_0 the measurement limit in small scales $x \to 0$.

An alternative way of obtaining the same family of generic cross-over models [2] exploits the simple argument of the parametrizable distribution of a nearly Gaussian shape which, when convolved with the ideal cross-over, leads to a particularly simple

[a] of course the cross-over length is of infinite width in this model; by effective cross-over length one can consider e.g. 3σ width of the corresponding distribution, the role of the distribution will become clear in the following.

model. The arguments for introducing stochastic distributions in the context of dimension measurement on deterministic fractal shapes are in fact not limited to the handy derivation of a crossover function family. In Fig. 2, we illustrate the results of an example measurement with the yardstick method on a reference deterministic shape (von Koch polygon). The evident phenomenon taking place is the appearance of an oscillatory behaviour vanishing towards the Euclidean region of small scales. The appearance of this 'artifact' is closely related to the regular renormalisation behaviour of the investigated deterministic sample. [2,3]

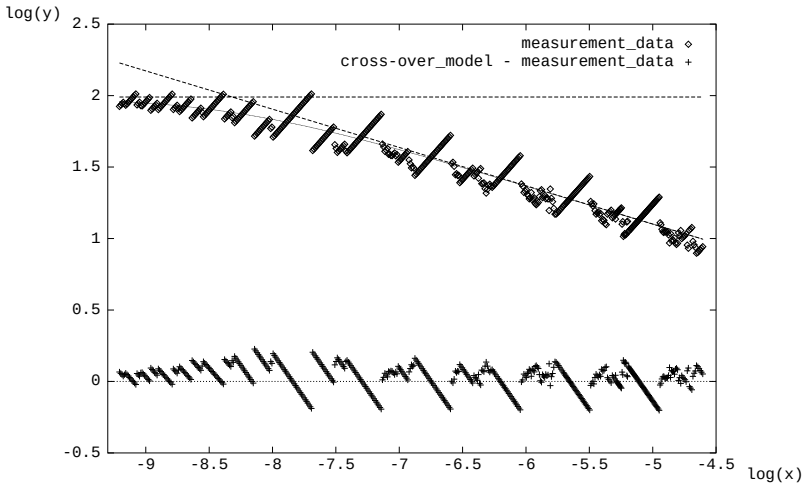

Figure 2: In the upper part of the figure the actual measurement is shown together with the fitted cross-over function and its asymptotes. Subtraction of the 'trend' defined as the cross-over function from the measurements gives the oscillatory part of the measurements shown below.

Fitting a generic crossover model to this (oscillatory) data is possible provided the scaling range in the sample is sufficiently large. However, the test shapes used for evaluating the parameter estimation with the nonlinear model fitting are deterministic fractals (von Koch polygon) of a low generation level (down to the range of two generations). Fitting the generic model to measurement results from such small generation levels would be impossible. Evaluation of the small generation levels was obtained using the 'fuzzy yardstick' method. [2] Roughly spoken, the method assumes the yardstick to be working at non-fixed scales due to some predefined length distribution obtained by superimposing 'noise' on the yardstick length. Whether this distribution of scales comes from the irregular character of the renormalisation inherent to the fractal object (e.g. in case of fBm) or is arbitrarily introduced is not primarily an issue here (although we will assume the latter).

If we consider the result of the measurement $Y(X)$ as a function of the random scale variable X, the expectation of $Y(X)$ is

$$E(Y) = \int_{-\infty}^{\infty} Y(X)\, g_{X_0,V_0}(X)\, dX \ , \tag{3}$$

where $g_{X_0,V_0}(x)$ is a certain distribution (details of how to choose the shape of this distribution will be given below) with mean X_0 and variance V_0. We can also

represent $E(Y(X))$ with respect to the distribution $g_{0,V_0}(X)$ around $X_0 = 0$, in which case Eq. 3 becomes the correlation of the two:

$$E(Y(X_0)) = \int_{-\infty}^{\infty} Y(X + X_0)\, g_{0,V_0}(X)\, dX \ . \tag{4}$$

Assuming a symmetrical distribution $g_{0,V_0}(X) = g_{0,V_0}(-X)$, on substituting $X' = X + X_0$ we can interpret Eq. 4 as a convolution product of the measurement function $Y(X)$ and the probability distribution $g_{0,V_0}(X)$ of the scale parameter X.[b]

$$E(Y(X_0)) = \int_{-\infty}^{\infty} Y(X')\, g_{0,V_0}(X' - X_0)\, dX \ . \tag{5}$$

A straightforward choice for $g_{0,V_0}(X)$ would be a centered (mean $\mu = 0$) Gaussian distribution with σ^2 variance: $g_{0,V_0}(X) = \frac{1}{\sqrt{2\,\pi}\,\sigma}\, e^{\frac{-X^2}{2\,\sigma^2}}$.
Calculating the convolution $E(Y(X_0))) = Ideal_{bound}(X) * g_{0,V_0}(X)$ with a Gaussian distribution $g_{0,V_0}(X)$ results in a transition function Eq. 6, depicted together with its first derivative in Fig. 1.

$$E(Y) = b\left(\frac{X}{2} + \frac{X}{2}\,\mathrm{erf}(\frac{1}{\sqrt{2}}\,\frac{X}{\sigma}) + \frac{\sigma}{\sqrt{2\,\pi}}\, e^{-\frac{1}{2}\,\frac{X^2}{\sigma^2}}\right) \ , \tag{6}$$

where the error function $\mathrm{erf}(x) = 2/\sqrt{\pi}\, \int_0^x \exp(-t^2)$.

As was to be expected, the cross-over now takes a finite width (as opposed to being singular in Eq. 1) and its character is fully determined by the function $g(X)$ regardless of the b value of the asymptotic slope of the fractal regime. Different σ give a different width to the cross-over region. The function Eq. 6 unfortunately has a rather inconvenient form. However, if we use a slightly different distribution of the form given by Eq. 7,

$$g(X) = \frac{a}{4}\, \frac{1}{\cosh^2\left(\frac{a\,X}{2}\right)} \tag{7}$$

for the centered version, with variance $\pi^2/3\,a^2$, the transition function takes a particularly simple form:

$$E(Y) = \frac{b}{a}\, \log(\exp(a\ X) + 1) \ . \tag{8}$$

With the explicit upper limit y_0 and cross-over location x_c parameters in the length coordinates x, y, it reads

$$y(x) = y_0\, (x^a + x_c^a)^{b/a} \ . \tag{9}$$

To summarize, the key point in the parametric cross-over model presented is that the different a changes the 'fractional' powers $(.)^a$ and $(.)^{b/a}$ in Eq. 9, thereby affecting the shape of the cross-over but leaving the difference of the slopes of the asymptotes at value 'b'.

[b] This step is not necessary since formally we could simply proceed with the correlation product - yet the convolution product seems to lend itself more easily to an intuitive interpretation in this case.

2 Estimating the Multi-parameter Cross-over Model

The two (or more) sided model can be easily designed with the curvature parameter p as postulated in Eq. 9. For the two sided model, we have

$$y_p = y_0 \left(\frac{1 + (x/x_c)^{-bp}}{1 + (x/x_d)^{-bp}} \right)^{-1/p} . \tag{10}$$

The example fit can be seen in Fig. (3). Data is obtained from the fuzzy yardstick measurement of the von Koch polygon. For the purpose of better access to the lower transition region we used a sequence of several von Koch polygons 'embedded' in a straight line. Thanks to the fuzzy yardstick there are no oscillations in the data - they are 'converted' into the standard deviation of the data. Several other aspects previously discussed elsewhere [1,3] are visible, as the scaling of standard deviation and the obvious bias of the slope of any potential linear model fit to a selected data section, as compared to the asymptote obtained from the fit of the non-linear model as in Eq. 10.

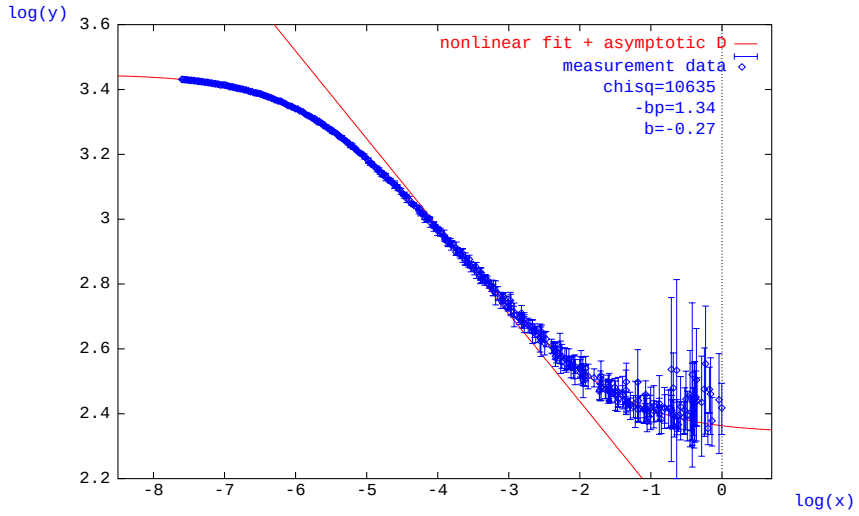

Figure 3: Fitting the double cross-over model with free curvature parameter p Eq. 10 to the data containing both upper and lower transition regions.

This can be further extended to independent curvatures for both transition regions. Let us first separate Eq. 10 into two cross-over regions

$$y_{double} = y_0 \left(1 + x/{x_c}^{-bp}\right)^{-1/p} \left(1 + x/{x_d}^{-bp}\right)^{1/p} . \tag{11}$$

It is immediately evident that

$$y_{double\ p} = y_0 \left(1 + x/{x_c}^{-bp_1}\right)^{-1/p_1} \left(1 + x/{x_d}^{-bp_2}\right)^{1/p_2} \tag{12}$$

can be used to fit two transition regions of different curvatures. Similarly more transition regions can be modeled:

$$y_{triple} = y_0 \left(1 + x/{x_c}^{-b_1 p}\right)^{-1/p} \left(1 + x/{x_d}^{-(b_2 - b_1)p}\right)^{1/p} \left(1 + x/{x_e}^{b_2 p}\right)^{1/p} . \qquad (13)$$

Unfortunately, with each such step at least one extra parameter is introduced which makes fitting extended models of this kind very expensive and prone to becoming stuck in local minima while optimizing the fit to real data. This fact, already mentioned above, is addressed again since we would like to demonstrate the practical approach of fitting the many parameter model by using one of the free parameters as the control value.

We have already examined one of the simplifying cases: fixing a curvature parameter a based on several observations or *a priori* knowledge. Here we would like to introduce an approach aiming at the estimation of the realistic error bound on the dimension parameter D, through identifying confidence intervals. For the non-linear fit of many parameters, the usual approach is the Monte Carlo sampling of the parameter space $\{param.\}$.[4] Due to the special role of the parameter $-bp$, we chose in our approach for the deterministic section through the $\{\chi^2(param.)\}$ space along the optimal fit for a given value of the curvature parameter $-bp$. As will be duly demonstrated, this gives insight into the stability of the fit and the estimated parameter b and gives the means to obtain realistic confidence intervals.

In the example of the fourth generation of the von Koch curve below, the main idea of this approach is made clear - fixing the curvature parameter $-bp$ in order to perform the usual non-linear fit to data of the reduced model. This is done for values of parameter $-bp$ from a preselected range (around χ^2_{min}). The resulting goodness of fit and estimated parameter b are next plotted as functions of $-bp$ as demonstrated in Fig. 4.

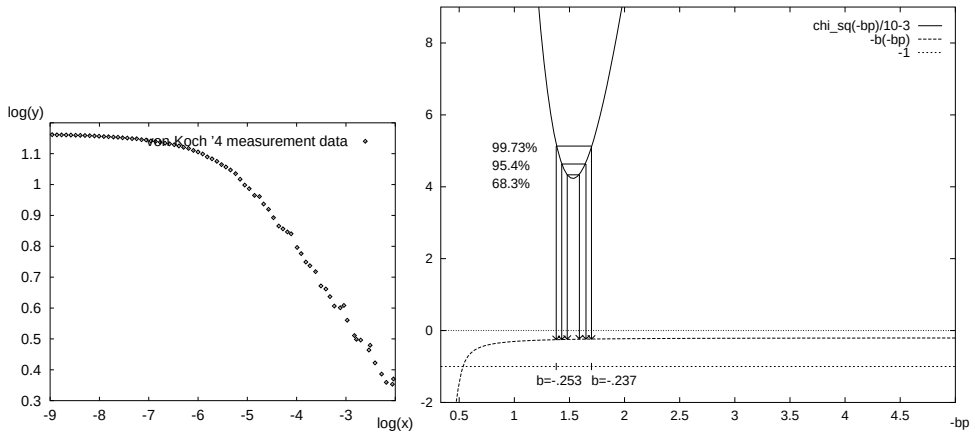

Figure 4: In this figure the parameter $-bp$ varies from $-bp = 1/3$ to $-bp = 5$ and the values of $\chi^2(-bp)/10 - 3$ and $-b(-bp)$ are shown for the yardstick measurement on the fourth generation of the von Koch curve shown in the left figure.

In this figure, the parameter p varies from $p = 1/3$ to $p = 5$ and the values of $\chi^2(-bp)$ and $b(-bp)$ are shown for the fuzzy yardstick measurement on the 4-th generation of the von Koch curve. The minimum of $\chi^2(-bp)$ falls at value $-bp$ which relates

to the close to the theoretic value of $b = \log(4)/\log(3) - 1 = 0.26....$ At confidence level of 3σ of χ^2 distribution,[c] which is 99.73% of the probability, we obtain the interval $[b = -0.253, b = -0.237]$. Lower than the $b = \log(4)/\log(3) - 1 = 0.26...$, this is no surprise due to the relatively low generation level of the pre-fractal and, therefore, the 'scaling range' limited to less than two decades.

Even for the relatively small scaling range, there are reasons to claim that the fit is *stable* and there are grounds for taking the estimated scaling exponent seriously. The fact that the fit is stable is reflected in the almost constant behaviour of the $b(-bp)$ parameter value in the vicinity of the minimum of $\chi^2(-bp)$. Indeed, in the tests we performed with lower levels of development of the von Koch polygon, the position of the minimum of $\chi^2(-bp)$ was strictly related to the generation level. For smaller generation levels, the minimum of $\chi^2(-bp)$ was to be found closer to the strongly non-linear part of $b(-bp)$, resulting in larger error bounds on b for the same deviation from the minimum of $\chi^2(-bp)$. For an illustration in the case of the second generation level of the von Koch pre-fractal, see Fig. 5.

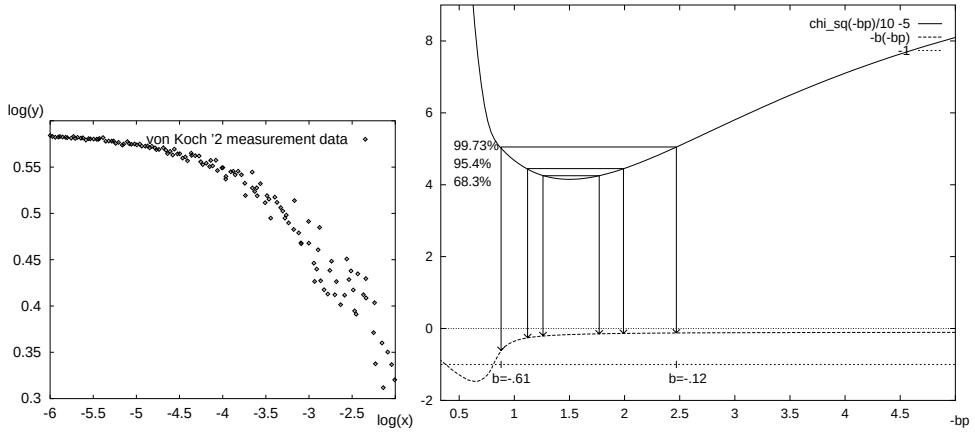

Figure 5: In this figure the parameter $-bp$ varies from $-bp = 1/3$ to $-bp = 5$ and the values of $\chi^2(-bp)/10 - 9$ and $-b(-bp)$ are shown for the yardstick measurement on the second generation of the von Koch curve shown in the left figure.

For both the above examples, the variance of the measurements was estimated from the value of the minimum of χ^2 for the best non-linear fit. Although sometimes the only one available, usually this is a rather optimistic estimate.

Using the noisy yardstick method and running one hundred experiments, we obtained somewhat better statistics and a more realistic estimates of the actual variance. The effect of these in the case of the second generation level of the von Koch curve is presented in Fig. 6 below.

At the minimum of χ^2, the interval of b at 68.3% confidence contains b between $[-0.34, -0.16]$. The 95.4% level of confidence covers practically all meaningful slopes! Although the fitting of the model to this data is quite legitimate, there are

[c]Note, that these levels have only historical meaning. We do not require the distribution of the errors to be Gaussian - the χ^2 fitting procedure is robust in most cases although it is the maximum likelihood estimate in the Gaussian case.

no grounds for speaking of any scaling exponent or fractal behaviour whatsoever.

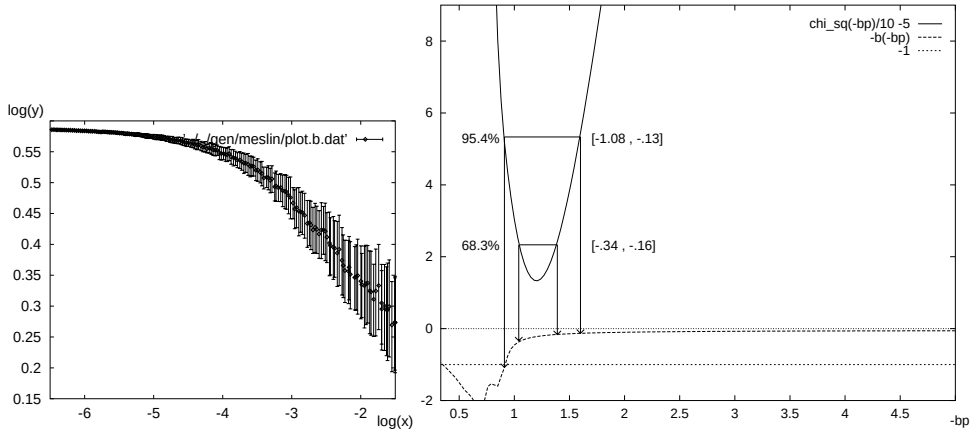

Figure 6: In this figure the parameter $-bp$ varies from $-bp = 1/3$ to $-bp = 5$ and the values of $\chi^2(-bp)$ and $-b(-bp)$ are shown for the results of 100 measurements (shown in the left figure) using noisy yardstick on the von Koch curve of 2-th generation level. With 95.4 confidence one cannot assign any physically meaningful scaling exponent to this measurement!

However, if the generation level of the Koch curve is high, a similar procedure involving fifty measurements and a parameterized non-linear fit, leads to a stable result at high confidence. See Fig. 7 for the example with 6-th generation of the von Koch curve. The extent of scaling region is over two decades.

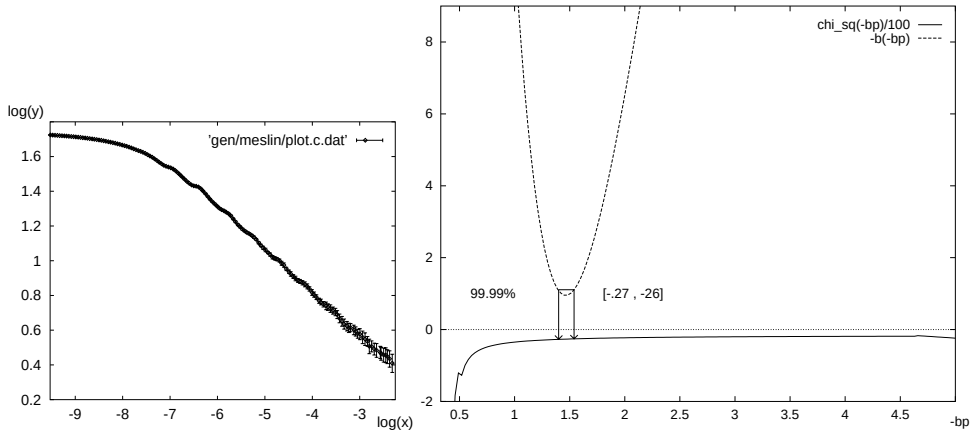

Figure 7: In this figure the parameter $-bp$ varies from $-bp = 1/3$ to $-bp = 5$ and the values of $\chi^2(-bp)/100$ and $-b(-bp)$ are shown for the results of 50 measurements (shown in the left figure) using noisy yardstick on the von Koch curve of 6-th generation level. At 99.99% confidence level the scaling exponent b is in the interval $[-0.27\ ,\ -0.26]$

In the test we performed on real handwriting patterns, we observed similar effects as in the case of the low generation level of the von Koch curve. In the first example below, the minimum of $\chi^2(-bp)$ is found over the strongly non-linear region of

$b(-bp)$, leading to relatively high error bound for a small deviation from the minimum of $\chi^2(-bp)$. However, for small deviations, the estimated value still remains below the upper bound, the topological dimension 2, which is equivalent to $b = -1$, as indicated in Fig. 8.

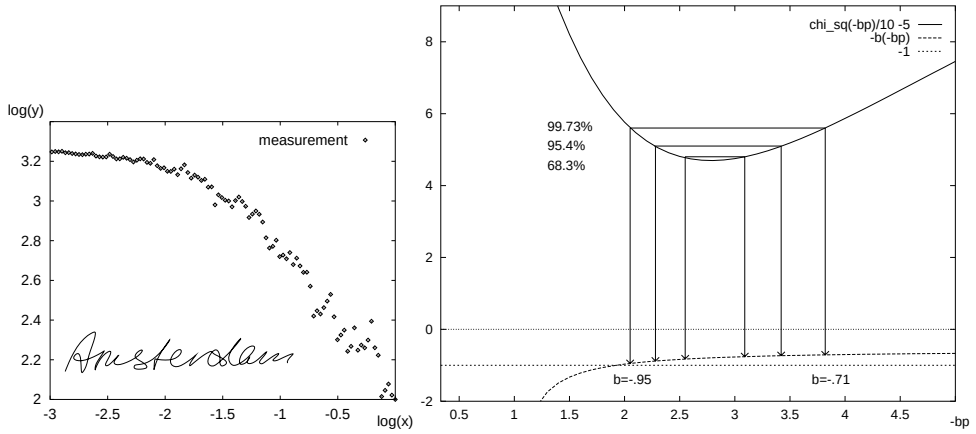

Figure 8: In this figure the the parameter $-bp$ varies from $-bp = 1/3$ to $-bp = 5$ and the values of $\chi^2(-bp)/10 - 5$ and $-b(-bp)$ are shown for the yardstick measurement on the handwriting sample shown in the left figure.

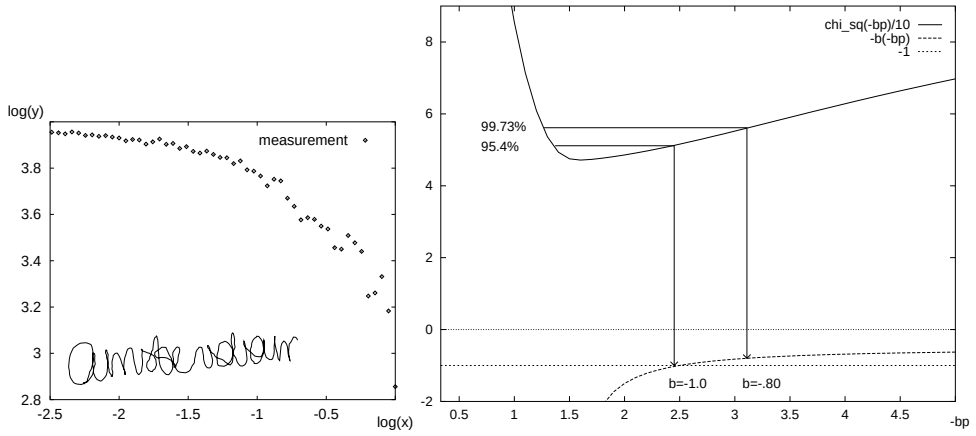

Figure 9: As above with a different handwriting sample.

This is not the case in the second example, see Fig. 9; the minimum of $\chi^2(-bp)$ is not only located over a highly non-linear region of $b(-bp)$, it is also above the $b = -1$ bound of physical plausibility. In this case there are no indications for defending the null hypothesis of the presence of fractal scaling of the investigated pattern. Indeed, the extent of the 'scaling range' is much less than a decade in this example, while the rule of thumb favoured by fractologists refers to the minimum of one decade of scaling to give any meaning to the exponent.

We conclude by indicating that the method outlined above gives practical means of achieving insight into the grounds for proving the fractal nature of objects for

which scaling is to be found on a very limited range of scales. In the first of the handwriting test examples presented above, the scaling estimate, though very unreliable, can be sought. This is a genuine piece of male human writing with patterns to be found on several length scales. The second sample is a piece of female handwriting and contains very limited variation of scale dependent patterns. The hypothesis of fractal scaling has no grounds, as indicated through outlined analysis.

3 Conclusions

One can adopt the possibility to fit a generic model of the kind introduced here as the criterion replacing the 'fitting of the straight line' test for fractality. Contrary to this commonly exercised approach, fitting the generic cross-over model accommodates the transition between fractal and Euclidean regions - an unavoidable feature of scaling phenomena constrained in scale as they are in all real world situations. The benefits are primarily twofold.

First, the nonlinear bias on the measurement data which is usually neglected and averaged, is eliminated through incorporating it in the more appropriate, nonlinear cross-over model. The entire investigated scale domain is treated on an equal base, therefore avoiding the purely *arbitrary* selection of the range of 'fractal' scaling for the linear fit routinely performed. In effect, this avoids the influence of the unavoidable bias [1] on the estimated value of $D = 1 - b$ due to fitting the wrong model, or taking arbitrary and uncontrollable linear approximations.

There is naturally the second aspect of fitting the more appropriate model, namely the more trustworthy estimate determination of the confidence limits on estimated parameters of the model (including the *asymptotic* scaling parameter b). This, in turn, can be used for testing the hypothesis as to whether the estimated scaling belongs to the class of fractally scaling phenomena. In other words, the fact whether the investigated object is a *fractal* can be verified.

In some cases, the parameters obtained can give some insight into the physics of the scaling phenomena through e.g. the estimates of the upper and lower cross-over points. The fractional power p - the *transition speed* between the Euclidean and fractal regions, may also provide information on the *physical* model of the investigated phenomenon.

References

1. Z.R. Struzik, E.H. Dooijes, Towards Fractal Metrology, in M.M. Novak, ed., *Fractals in the Natural and Applied Sciences*, North-Holland (1994).
2. Z.R. Struzik, E.H. Dooijes, Experimental Determination of the Fractal Dimension of a Deterministic Fractal, Tech. Rep. No.: CS-93-03 (rev.94) Univ. of Amsterdam (1994).
3. Z.R. Struzik, From Coastline Length to Inverse Fractal Problem: The Concept of Fractal Metrology, *Thesis*, University of Amsterdam, (1996).
4. W.H. Press, B.P. Flannery, S.A. Teukolsky, W.T. Vetterling, *Numerical Recipes - The Art of Scientific Computing*, Cambridge University Press (1986).